Pancreatic Endocrine Tumors: Tumor Blood Flow Assessed with Perfusion CT Reflects Angiogenesis and Correlates with Prognostic Factors[1]

Gaspard d'Assignies, MD
Anne Couvelard, MD
Stéphane Bahrami, MD
Marie-Pierre Vullierme, MD
Pascal Hammel, MD
Olivia Hentic, MD
Alain Sauvanet, MD
Pierre Bedossa, MD
Philippe Ruszniewski, MD
Valérie Vilgrain, MD

Purpose: To prospectively correlate multidetector computed tomographic (CT) perfusion measurement of pancreatic endocrine tumors with tumor microvascular density (MVD) assessed by using histologic techniques and to determine whether perfusion CT parameters differ between tumor grades.

Materials and Methods: Institutional review board approval and informed consent were obtained. Thirty-six patients (15 men, 21 women; mean age, 53 years; range, 18–78 years) with resectable pancreatic endocrine tumors underwent presurgical dynamic perfusion CT. Twenty-eight (78%) of 36 patients were included in the study group; eight were excluded because of artifacts that were not compatible with perfusion postprocessing. Multidetector CT perfusion data were analyzed to calculate tumor and normal pancreatic blood flow, blood volume, mean transit time, and permeability–surface area product. Multidetector CT perfusion parameters were compared with intratumoral MVD by using the Spearman correlation coefficient and with World Health Organization (WHO) classification, tumor size, tumor proliferation index, hormonal profile, and presence of metastases by using Mann-Whitney tests.

Results: High correlation ($r = 0.620$, $P < .001$) was observed between tumor blood flow and intratumoral MVD. Blood flow was significantly higher ($P = .02$) in the group of benign tumors (WHO 1) than in the groups of tumors of indeterminate prognosis (WHO 2) or well-differentiated carcinomas (WHO 3). Blood flow was significantly higher in tumors with a proliferation index of 2% or less ($P = .005$) and in those without histologic signs of microscopic vascular involvement ($P = .008$). Mean transit time was longer in tumors with lymph node ($P = .02$) or liver ($P = .05$) metastasis.

Conclusion: Perfusion CT is feasible in patients with pancreatic endocrine tumors and reflects MVD. Perfusion CT measurements are correlated with histoprognostic factors, such as proliferation index and WHO classification.

[1] From the Departments of Radiology (G.d.A., M.P.V., V.V.) and Pathology (A.C., P.B.), INSERM Unité 773 CRB3 (A.C., P.B., V.V.), and the Fédération Médico Chirurgicale (P.H., O.H., A.S., P.R.), Beaujon Hospital, 100 boulevard général Leclerc, 92110 Clichy La Garenne, France; and Department of Epidemiology, Biostatistics and Clinical Research, Hôpital Bichat, APHP, University of Paris 7, Paris, France (S.B.). Received February 12, 2008; revision requested May 1; revision received June 17; accepted July 3; final version accepted July 22. Supported by a grant from the Roche Foundation. **Address correspondence to** G.d.A. (e-mail: *gdassignies@gmail.com*).

While pancreatic endocrine tumors are mostly well differentiated, the aggressiveness and growth patterns vary greatly, from nearly benign to highly malignant. Various clinicopathologic features have been identified to help distinguish pancreatic endocrine tumors with benign, indeterminate, or highly malignant growth patterns. Prognostic indicators that were developed in the revised World Health Organization (WHO) classification (1,2) include the presence of metastases (hepatic and nodal); tumor differentiation (3,4); tumor size; the presence and type of hormonal hypersecretion; signs of microscopic vascular neoplastic involvement (5); and markers of cell proliferation, such as the mitotic index and the expression of the cell cycle–associated Ki-67 antigen by using the MIB-1 monoclonal antibody (6). However, despite the use of these indicators, a large group of tumors remain without clear assessment of malignancy risk at the time of diagnosis.

Tumor growth is highly dependent on the development of a vascular supply, and blood vessel growth regulators have been shown to play a key role in the progression of many tumors (7). Like normal endocrine tissue, endocrine tumors often have a dense capillary network (8). This high vascular density results in the characteristic enhancement feature, which has been described at contrast material–enhanced computerized tomography (CT) (9–11). Microvascular density (MVD), evaluated by counting vessels on tissue specimens, is the standard technique used to quantify angiogenesis in histologic studies (12). MVD has been shown to have prognostic value in pancreatic endocrine tumors (13–15). The analysis of MVD in these tumors may help identify patients with an unfavorable prognosis (13), despite the presence of other favorable conventional histoprognostic factors in these lesions. This is of considerable importance because tumors with poorer prognosis according to WHO criteria are treated more aggressively than those with better prognosis. However, MVD analysis requires postoperative tumor tissue, so it is not practical for long-term ongoing patient monitoring (16,17).

A recent retrospective study (18) showed an association between MVD and semiquantitative degrees of tumor enhancement by using contrast-enhanced helical CT, which suggests that this technique could help differentiate tumor grades.

The relationship between CT-measured contrast medium enhancement and contrast medium blood concentrations allows quantification of the following four functional parameters by using a perfusion CT technique: blood flow, vascular blood volume, vascular mean transit time, and vascular permeability–surface area product (17,19). Perfusion CT results provide reliable quantitative tissue perfusion measurement and have been evaluated in various tumors for the quantification of angiogenesis (20–22).

Thus, the purpose of this study was to prospectively correlate multidetector CT perfusion measurement of pancreatic endocrine tumors with tumor MVD assessed by using histologic techniques and to determine whether perfusion CT parameters differ between tumor grades.

Advances in Knowledge

- Tumor blood flow assessed with CT perfusion was strongly correlated with intratumoral microvascular density at histologic examination ($r = 0.620$, $P < .001$).
- Blood flow values of benign tumors (284 mL/100 g/min) were found to be distinct ($P = .02$) from tumors of uncertain behavior (229.1 mL/100 g/min) and well-differentiated carcinomas (153.5 mL/100 g/min).
- Significant differences in tumor blood flow and mean transit time were observed on the basis of histoprognostic factors: proliferation index ($P = .005$) for blood flow, microscopic vascular neoplastic involvement ($P = .008$) for blood flow and mean transit time, and presence of lymph node ($P = .02$) or liver ($P = .05$) metastasis for mean transit time.

Implications for Patient Care

- Perfusion CT could help in therapeutic decision making by providing additional preoperative information about tumor grade.
- In patients with small pancreatic tumors located in the head, where benefit of surgery has not been proved, favorable perfusion parameters could favor follow-up rather than an aggressive approach.
- Perfusion CT might help to monitor response to novel therapies, such as antiangiogenic drugs.

Materials and Methods

The study was approved by the Institutional Review Board of Beaujon Hospital, and informed consent was obtained from each participant before the study. This study was supported by a grant from the Roche Foundation. Financial support was given and used for histopathologic analysis. The authors had full control of the data and information submitted for publication.

Patients

Inclusion criteria included the following: *(a)* patients with pancreatic endocrine tumors that were diagnosed on the basis of evidence of hormonal hypersecretion (chromogranin A), specific imaging

Published online before print
10.1148/radiol.2501080291

Radiology 2009; 250:407–416

Abbreviations:
MVD = microvascular density
ROI = region of interest
WHO = World Health Organization

Author contributions:
Guarantors of integrity of entire study, G.d.A., A.C., M.P.V., V.V.; study concepts/study design or data acquisition or data analysis/interpretation, all authors; manuscript drafting or manuscript revision for important intellectual content, all authors; manuscript final version approval, all authors; literature research, G.d.A., A.C., M.P.V., P.R.; clinical studies, G.d.A., A.C., M.P.V., P.H., O.H., A.S., P.B., P.R., V.V.; statistical analysis, S.B.; and manuscript editing, G.d.A., A.C., A.S., P.R., V.V.

See Materials and Methods for pertinent disclosures.

features (positive finding at somatostatin-receptor scintigraphy), and/or results of tumor biopsy and *(b)* indication for surgical resection, including patients with potentially resectable liver metastases. All patients underwent perfusion CT as part of their presurgical work-up. The mean delay from examination to surgery was 53 days (range, 3–72 days).

From September 2005 to July 2007, 36 patients (15 men, 21 women; mean age, 53 years; range, 18–78 years) were prospectively included. Twenty-eight (78%) of these 36 patients were ultimately included in the study group. Eight were excluded after consensus evaluation by two radiologists (G.d.A., 5 years of experience in radiology; M.P.V., 20 years of experience in gastrointestinal radiology) because of motion and beam-hardening artifacts, which severely limited postprocessing of multidetector CT data. The mean age at resection was 53 years (range, 18–78 years). Mean age was 55 years (range, 32–78 years) in the female group and 50 years (range, 18–74 years) in the male group. Ten (36%) patients presented with clinical evidence of a functional hormonal syndrome, which was related to insulin hypersecretion in six cases, gastrin hypersecretion in two cases, and glucagon hypersecretion in two cases. All clinical data were reported by one clinician (P.R., 25 years of experience in gastroenterology) after review of patient records.

Perfusion CT Technique

Perfusion CT was performed with a 64-section multidetector CT scanner (LightSpeed VCT; GE Medical Systems, Milwaukee, Wis).

An unenhanced multidetector CT abdominopelvic series (section reconstruction, 2.5 mm; section interval, 2.5 mm; speed, 27.5 mm per rotation; 120 kV; automatic tube current; 0.6-second rotation speed; field of view, 45 cm; and 512 matrix size) was initially obtained. On the basis of the unenhanced image, a supervising radiologist (M.P.V.) selected a perfusion CT volume that covered a 4-cm length in the z-axis, which was centered on the pancreatic tumor. A pump injector (Medrad, Pittsburgh, Pa) was used to inject 40 mL of intravenous nonionic contrast medium at 350 mg iodine per milliliter (iobitridol, Xenetix; Guerbet, Aulnay-sous-bois, France) through an 18-gauge catheter at a rate of 4 mL/sec.

The following CT acquisition parameters were used to acquire perfusion data: 1-second gantry rotation time, 100 kVp, 100 mA, acquisition in 8i transverse mode (eight sections per gantry rotation), 5-mm reconstructed section thickness, 512 matrix size, and 25-mm field of view. Scanning was initiated 5 seconds after the injection began, and images were acquired every second for the first 30 seconds and then every 3 seconds for 2 minutes.

Patients were asked to breathe quietly during the examination to minimize motion artifacts.

The perfusion CT examination resulted in an additional effective dose of 10 mSv to the patients.

After the perfusion study, diagnostic arterial and portal venous phase abdominopelvic multidetector CT was performed at 25–35 seconds and at 60–70 seconds, respectively, after the initiation of another intravenous injection (volume, 1.5 mL per kilogram of body weight − 40 mL; rate, 3 mL/sec). The following scanning parameters were used: section reconstruction, 1.25 mm; section interval, 1.25 mm; speed, 39.37 mm per rotation; 120 kV; automatic tube current; 0.6-second rotation speed; field of view for arterial phase, 25 cm; field of view for portal venous phase, 40 mm; and 512 matrix size.

Imaging Data Analysis

Images obtained during the arterial and portal venous phases were interpreted for morphologic data in consensus by two abdominal radiologists (M.P.V.; V.V., with 21 years of experience in radiology).

Tumor size, cystic components, calcification, dilatation of the main pancreatic duct, and vascular involvement were recorded. Tumor enhancement relative to the surrounding pancreatic parenchyma on contrast-enhanced arterial phase images was noted as hyperattenuating, isoattenuating, or hypoattenuating. Suspicion of liver and lymph node metastases was recorded and confirmed intraoperatively by using ultrasonography and histologic analysis of biopsy or resected specimens.

Perfusion data were processed at a workstation (Advantage Windows, version 4.4; GE Medical Systems) with perfusion CT software (Perfusion, version 4.0, research mode; GE Medical Systems) by a radiologist (G.d.A., with 5 years of experience in radiology and 1 year of experience in gastrointestinal radiology and perfusion CT software) who was not aware of histologic and clinical data. The perfusion model used in this software is based on a distributed version of a compartmental model (17,23), which was developed with capillary permeability in consideration, as reported by Johnson and Wilson (24). This model allows simultaneous determination of blood flow (in mL/100 g/min), blood volume (in milliliters per 100 g), mean transit time (in seconds), and permeability–surface area product (in mL/100 g/min).

The arterial input was determined by manually placing a circular region of interest (ROI) on the abdominal aorta (range, 40–167 mm^2). An arterial time-enhancement curve for the 120-second acquisition time was generated automatically, as well as parametric maps of blood volume, blood flow, mean transit time, and permeability.

An ROI was then drawn within the greatest tumor dimension plane of the pancreatic tumor (range, 11–564 mm^2). If homogeneous enhancement was found, the ROI was drawn to cover at least 50% of the tumor surface. If heterogeneous enhancement was found, the area with the highest enhancement was selected. Care was taken to avoid regions of tumor calcification, necrotic areas, and adjacent normal vasculature.

On each image where motion artifacts were present, the software allowed for manual relocation of the ROI to keep it in the tumor region.

ROIs were also drawn in the adjacent pancreatic parenchyma when seen on perfusion images (n = 18; range,

12–126 mm^2). ROIs were located downstream and distant to the tumor to avoid possible obstructive pancreatitis and away from normal vasculature. The ROI size should have been at least 12 mm^2. The 40-mm coverage of perfusion CT acquisition did not allow us to explore the normal pancreatic parenchyma because of large tumors in 10 cases.

A tissue time-enhancement curve and the four perfusion parameters (blood volume, blood flow, mean transit time, and permeability) were derived automatically for selected ROIs. ROI values for the four perfusion parameters were recorded for each patient.

Histopathologic Analysis

Surgical procedures and findings were recorded in the patient report by a surgeon (A.S., 23 years of experience in abdominal surgery) involved in the study.

Macroscopy and microscopy.—After 24 hours of fixation in formalin, the tumors were sliced axially to facilitate comparison with perfusion CT images.

Tissue slices (4 μm) from paraffin-embedded blocks containing the tumor and the peripheral nontumoral pancreas (when possible in large pancreatic resections; $n = 21$) were cut and stained with hematoxylin-eosin. Many representative tissue blocks were taken and analyzed, especially those that corresponded to the area of the greatest tumor diameter (area sampled in one to eight blocks, depending on the size of the tumor). Tumors were classified as endocrine with histologic examination of the hematoxylin-eosin staining and with immunohistochemical expression of both chromogranin (clone DAK-A3; Dako, Carpinteria, Calif) and synaptophysin (clone SY38; Dako). For each case, the following features were recorded by a pathologist (A.C., 15 years of experience): tumor differentiation, size, presence of necrosis, evidence of vascular neoplastic involvement, presence of regional lymph node metastasis, number of mitoses per 10 high-power fields, and evaluation of the Ki-67 proliferation index. The latter was performed by using immunohistochemistry with the MIB-1 antibody (Dako) by using an automatized technique (streptavidin peroxidase with an automated immunostainer [Benchmark; Ventana, Illkirch, France]) in a selected block for each tumor in the area of highest staining, according to Rindi et al (6).

Tumors were classified into three groups according to the WHO 2000 criteria: Well-differentiated endocrine tumors of benign behavior were noted as WHO 1, well-differentiated endocrine tumors of uncertain behavior were noted as WHO 2, and well-differentiated endocrine carcinomas were noted as WHO 3 (1,2). There were no poorly differentiated endocrine carcinomas (WHO 4) in this study.

Assessment of MVD.—Quantification of MVD was performed after immunostaining with a CD34 antibody (QBEND10; Immunotech, Marseille, France) by using an automatized technique (streptavidin-peroxidase with an automated immunostainer [Benchmark; Ventana]) in all blocks taken from the greatest tumor diameter and also in a block corresponding to normal pancreas (without any fibrosis or pancreatitis) taken at a distance from the tumor. In tumors, the area of highest vascularization (hot spot) was chosen for microvessel counting at low magnification (×10 objective) among all the blocks that were immunostained.

Assessment of vascularity was performed by calculating the percentage of area of vessels, which reflects MVD. This was calculated as the percentage of four 40× field areas (total surface, 1 mm^2) occupied by the vessels. This was assessed by point counting by using a Mertz eyepiece graticule that contained 100 points. Vessels coinciding with the points were counted, and the result was expressed as a percentage of area.

Statistical Analysis

Perfusion parameters were expressed by their mean and median and interquartile range because the distribution was skewed. Paired pancreatic tumor and normal pancreatic perfusion values were compared by using Wilcoxon tests. The association between each of the four perfusion parameters and tumor MVD assessed with histologic techniques was estimated by using the Spearman correlation coefficient. Finally, associations between these four perfusion parameters and histoprognostic factors or WHO classification were checked by using Mann-Whitney tests.

The thresholds were chosen according to the WHO classification criteria (Ki-67 proliferation index, 2%; tumor diameter, 2 cm).

A secondary analysis of the Ki-67 variable was performed with a 5% threshold because it is known to be of prognostic value (3). We chose to analyze the WHO 1 data versus WHO 2 and WHO 3 data because we thought differentiation between benign tumors and indeterminate or malignant tumors to be the most relevant information for patient care. All other analyses regarding the WHO classification variable were considered secondary.

A P value of .05 or less was considered to indicate a significant difference. Statistical tests for secondary analyses were reported and interpreted only when primary tests showed significant results. In addition, Bonferroni adjustment for multiple testing was applied to secondary tests regarding the WHO classification variable.

Data were analyzed by using software (SAS, version 9.1; SAS Institute, Cary, NC).

Results

Clinical and Radiologic Patient Characteristics

The median diameter of the tumor at CT examination was 20 mm (range, 8–130 mm). Tumors appeared as homogeneous solid masses in 12 (43%) of 28 cases. Cystic components were found in three (11%) of 28 tumors, and calcification was found in four (14%) of 28 cases. Dilatation of the main pancreatic duct was found in six (21%) of 28 patients, and vascular involvement was found in seven (25%) of 28 patients. Tumor enhancement relative to the surrounding pancreatic parenchyma on contrast-enhanced arterial phase im-

ages varied for the 28 depicted tumors: 18 (64%) were hyperattenuating, seven (25%) were isoattenuating, and three (11%) were hypoattenuating. Liver metastases were seen in five (18%) patients. Abnormal lymph nodes with a diameter of more than 10 mm were seen in seven (25%) patients.

Surgical Procedures and Pathologic Characteristics

Six tumors were located in the head of the pancreas, three were located in the neck, and 19 were located in the body and/or tail. The following surgical procedures were performed: Whipple procedure in four (14%) patients, left pancreatectomy in 14 (50%) patients, isthmic resection in three (11%) patients, and tumor enucleation in seven (25%) patients. Tumor size ranged from 8 to 140 mm in largest diameter (median, 22.5 mm). Table 1 summarizes the relevant clinical and histologic patient characteristics.

Table 2 summarizes the comparison between MVD and clinical and histologic data. MVD ranged from 1 to 22 (median, 4.5; quartile range, 2.5). MVD was significantly higher in WHO 1 tumors than in WHO 2 and 3 tumors ($P = .015$), in smaller tumors (<2 cm in diameter) ($P < .01$), and in tumors with a lower (<2%) proliferation index ($P = .042$).

Perfusion Results

The comparison between pancreatic tumor and normal pancreas perfusion values are shown in Table 3. No significant difference was found; however, blood flow tended to be higher in tumors than in normal pancreas. In endocrine tumors, median blood flow, blood volume, mean transit time, and permeability–surface area product were 152 mL/100 g/min (quartile range, 198 mL/100 g/min), 21.3 mL/100 g (quartile range, 24.6 mL/100 g), 11 seconds (quartile range, 12 seconds), and 65.8 mL/100 g/min (quartile range, 90.7 mL/100 g/min), respectively.

Correlation between Perfusion Measurement and Intratumoral MVD

Tumor blood flow was strongly correlated with MVD ($r = 0.620$, $P < .001$).

Correlation between mean transit time and MVD was not significant ($r = -0.353$, $P = .065$), and no significant correlation was found between blood volume or permeability–surface area product and MVD.

Comparison between Tumor Perfusion Data, WHO Classification, and Histoprognostic Factors

Table 4 summarizes the comparison of perfusion measurements with clinical and histologic data. Mean tumor blood flow was significantly higher in WHO 1 tumors (Fig 1) than in WHO 2 and 3 tumors (Fig 2) ($P = .02$). No significant difference in blood flow was found between WHO 1 and WHO 2 tumors. With a blood flow threshold value of less than 86 mL/100 g/min, sensitivity and specificity of blood flow in the differentiation of well-differentiated carcinoma (WHO 3) from well-differentiated tumors (WHO 1 and 2) were 40% and 80%, respectively. With a threshold value of less than 250 mL/100 g/min, sensitivity and specificity were 85% and 40%, respectively.

Table 1

Clinical and Histologic Characteristics in 28 Patients with Pancreatic Endocrine Tumors

Parameter	Datum
Sex	
Male	11 (39)
Female	17 (61)
Multiple endocrine neoplasia type 1 disease	
Present	3 (11)
Absent	25 (89)
Functional syndrome	
Present	10 (36)
Absent	18 (64)
Tumor diameter	
<2 cm	11 (39)
≥2 cm	17 (61)
WHO classification	
WHO 1: benign tumors	9 (32)
WHO 2: tumors of uncertain prognosis	6 (21)
WHO 3: well-differentiated carcinomas	13 (46)
Ki-67 proliferation index	
≤2%	15 (54)
>2%	13 (46)
2%–5%	4 (14)
5%–15%	9 (32)
Microscopic vascular neoplastic involvement	
Present	13 (46)
Absent	15 (54)
Presence of metastases	
Liver	5 (18)
Lymph node	12 (43)*

Note.—Data are numbers of patients, with percentages in parentheses.

* Includes the five patients with liver metastasis.

Table 2

Comparison between MVD and Clinical and Histologic Data

Parameter	MVD	*P* Value
WHO classification		.015*
WHO 1 ($n = 9$)	6.8 (5.7) [3]	
WHO 2 ($n = 6$)	6.4 (3.7) [3]	
WHO 3 ($n = 13$)	3.7 (4.3) [2]	
Tumor diameter		.002
<2 cm ($n = 11$)	6.66 (5.5) [3]	
≥2 cm ($n = 17$)	4.46 (3.5) [2.2]	
Ki-67 proliferation index		.042
≤2% ($n = 15$)	6.7 (5) [4.5]	
>2% ($n = 13$)	3.7 (4) [1.2]	
<5% ($n = 19$)	6.2 (5) [3.5]	.046†
≥5% ($n = 9$)	3.3 (3.5) [2.4]	

Note.—Data are means, with medians in parentheses and quartile ranges in brackets.

* Comparison between WHO 1 and WHO 2 and 3 subgroup (primary analysis).

† Secondary analysis for 5% threshold.

Mean blood flow was significantly higher ($P < .001$) and mean transit time was significantly shorter ($P = .03$) in tumors less than 2 cm in diameter. In contrast, blood volume and permeability–surface area product were not significantly different in tumors of different size.

Mean tumor blood flow was significantly increased in tumors with a Ki-67 proliferation index of 2% or less ($P = .005$). Sensitivity and specificity of blood flow in the identification of tumors with a proliferation index of 2% or less were 87% and 62%, respectively, with a blood flow threshold value of more than 117 mL/100 g/min. Tumors with a proliferation index of less than 5% also had a significantly higher mean blood flow ($P = .005$).

There were no significant differences in mean transit time and permeability–surface area product parameters compared with proliferation index at the 2% threshold level.

Mean transit time was significantly longer in patients with lymph nodes with positive findings for metastatic disease ($P = .02$) or with hepatic metastases ($P = .05$) than in those without. Blood flow was relatively (but not significantly) lower ($P = .13$) in patients with liver metastases (median, 79 mL/100 g/min; quartile range, 77.8 mL/100 g/min) than in those without (median, 194 mL/100 g/min; quartile range, 174 mL/100 g/min).

Significantly lower blood flow ($P = .008$) and relatively higher mean transit time ($P = .07$) were found in tumors with evidence of microscopic vascular neoplastic involvement.

No difference in perfusion CT parameters was observed between tumors with or those without functional hormone syndrome.

Table 3

CT Perfusion Parameters in 18 Patients with Data Obtained from Endocrine Tumors and Normal Pancreas

Parameter	Tumor	Normal Pancreas	*P* Value
Blood flow (mL/100 g/min)	239.8 (183) [211]	130.4 (94.4) [111]	.06
Blood volume (mL/100 g)	23.9 (21.8) [24]	22.4 (23.3) [11.6]	.71
Mean transit time (sec)	10.9 (9.8) [11.3]	14.9 (18.2) [20.7]	.28
Permeability–surface area product (mL/100 g/min)	54.9 (55.3) [102]	32.4 (16.5) [64.8]	.14

Note.—Data are means, with medians in parentheses and quartile ranges in brackets.

Table 4

Comparison between Perfusion Measurement and Clinical and Histologic Data

Clinical and Histologic Data	Blood Flow (mL/100 g/min)	Blood Volume (mL/100 g)	Mean Transit Time (sec)	Permeability–Surface Area Product (mL/100 g/min)
WHO classification				
WHO 1 ($n = 9$)	284 (282) [152]	28.5 (21.10) [17.6]	8.1 (6) [8.9]	46.3 (52) [102]
WHO 2 ($n = 6$)	229.1 (99) [143.5]	14.7 (12.7) [6.2]	7.3 (7) [9]	71.8 (69.9) [50.1]
WHO 3 ($n = 13$)	153.5 (140) [161]	23.8 (21.5) [25]	13.9 (15) [15.2]	58.9 (68) [79.4]
P value (1 vs 2 and 3)	.02*	.18	.44	.40
Tumor diameter				
<2 cm ($n = 11$)	292 (282) [94]	24.5 (21.1) [27.7]	6.2 (4) [5.5]	60.3 (102) [102]
≥2 cm ($n = 17$)	159.8 (112) [71.2]	22.9 (21.5) [14.4]	13.6 (13) [6]	55.9 (63.6) [39]
P value	<.001	.93	.03	.57
Ki-67 proliferation index				
≤2% ($n = 15$)	282.7 (253) [173]	25.8 (23.5) [26.1]	8.4 (6) [12.3]	57.4 (68) [102]
>2% ($n = 13$)	129.9 (112) [98.5]	20.5 (16.6) [14.3]	13.3 (13) [12]	57.9 (63.6) [47.6]
P value	.005	.24	.19	.89
Lymph node metastasis				
Present ($n = 12$)	141.6 (126) [129.1]	25 (22) [23.5]	15 (15) [11.6]	55.3 (65.8) [81]
Absent ($n = 16$)	264 (216.5) [187]	22.2 (19.1) [20.2]	7.4 (5.5) [10]	59.3 (63.9) [84.5]
P value	.08	.54	.02	.79
Liver metastasis				
Present ($n = 5$)	122.8 (79) [77.8]	25.4 (19.2) [22.1]	19.5 (18.2) [13.4]	41.4 (22.6) [82.6]
Absent ($n = 23$)	236.5 (194) [174]	22.9 (21.3) [24.1]	8.6 (6.8) [10.9]	61.8 (68.6) [67]
P value	.13	.75	.05	.43
Angioinvasion				
Present ($n = 13$)	126.4 (112) [71]	22.9 (19.2) [24.7]	14 (13.9) [6]	51 (63.6) [48]
Absent ($n = 15$)	285.7 (253) [173]	23.7 (23.5) [24.1]	7.75 (5) [11.0]	63.4 (74) [102]
P value	.008	.81	.07	.35

Note.—Data are means, with medians in parentheses and quartile ranges in brackets.

* Results of secondary analyses for the blood flow parameter (after Bonferroni correction): WHO 1 versus 2, $P = .33$; WHO 1 versus 3, $P = .09$; WHO 1 and 2 versus 3, $P = .58$.

Discussion

Multidetector CT plays an important role in the diagnosis and staging of pancreatic endocrine tumors (11). Our results show that perfusion CT is a feasible technique to assess tissue perfusion in patients with endocrine tumors of the pancreas. This study also shows that tumor blood flow values are strongly correlated with intratumoral MVD and that perfusion parameters correlate well with a number of other prognostic indicators and thus may be of prognostic value.

The mean blood flow of endocrine tumors in our series (212 mL/100 g/min) is consistent with the reported results of other studies: Abe et al (25) found a blood flow value of 196.2 mL/100 g/min in one gastrinoma by using a

Figure 1

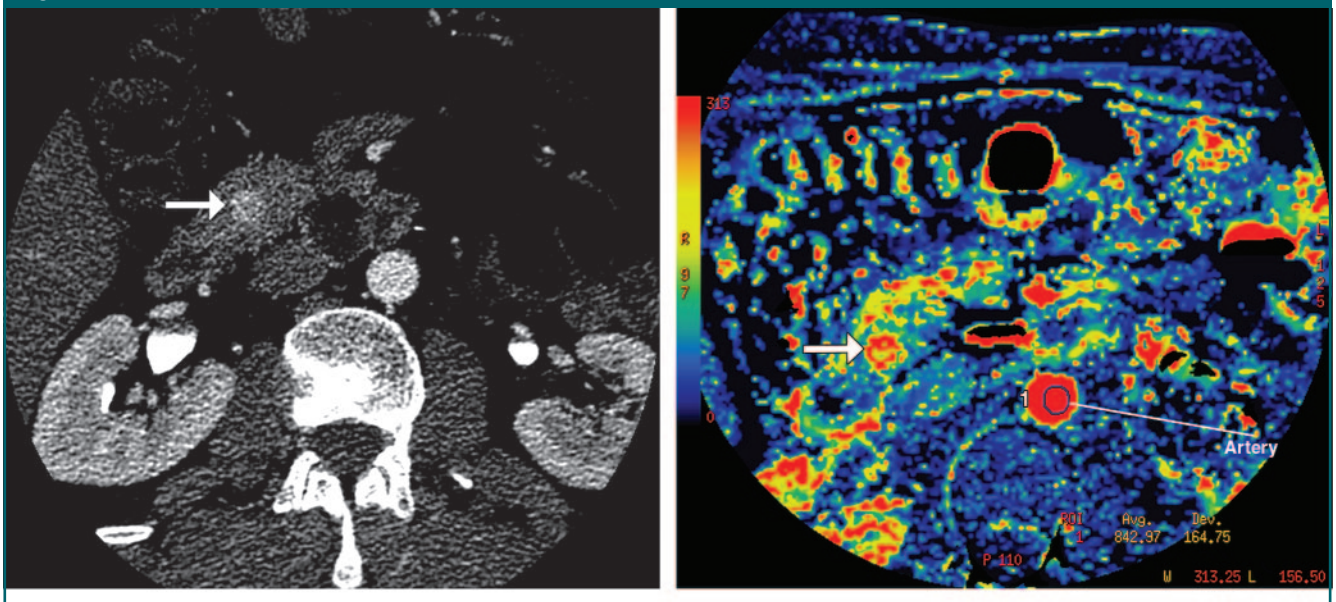

a. b.

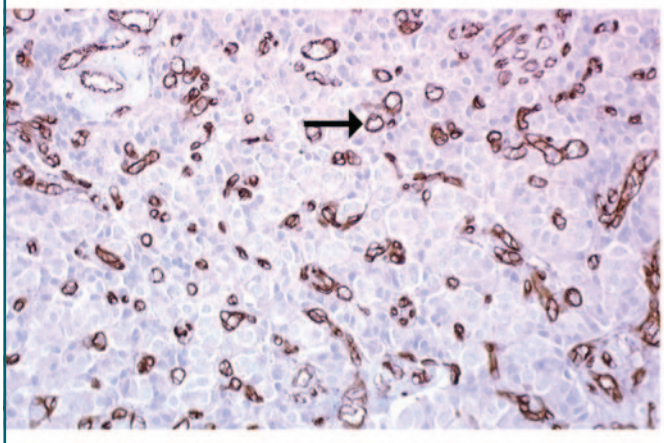

c.

Figure 1: Benign pancreatic endocrine tumor (WHO 1) in 44-year-old man. **(a)** Transverse contrast-enhanced CT image shows small enhancing mass in head of pancreas (arrow). **(b)** Functional CT perfusion color map of blood flow shows mass in pancreatic head with a distinct range of colors compared with the background pancreatic parenchyma (arrow). Blood flow in ROI drawn for the tumor was high (689 mL/100 g/min). **(c)** Immunostaining with CD34 antibody highlights vessels (arrow). Intratumoral MVD is high (13.5%). (Original magnification, ×200.)

deconvolution algorithm. Xue et al (26) observed a 206.5-mL/100 g/min mean blood flow value in 12 benign insulinomas by using the compartmental analysis method. In that study, blood flow, blood volume, and peak enhancement were found to be significantly different between normal pancreatic parenchyma in nine subjects and insulinoma in 12 subjects (26). In our series, there was no significant difference in blood flow, blood volume, mean transit time, and permeability–surface area product between tumors and normal parenchyma. This discrepancy between our results and those of Xue et al (26) may be due to the large variety of tumors in our study, which ranged from benign to highly malignant and resulted in a considerable variability in perfusion parameters.

Angiogenesis (ie, new capillary formation seen in neoplastic tissue) is being evaluated as a prognostic indicator in several types of cancer. Tumor angiogenesis is generally assessed by calculating MVD. The presence of high intratumoral MVD has been correlated with local invasion, the presence of metastases, and, in some series, with short survival of patients with carcinomas of the pancreas, colon, breast, and lung (27–30). Interestingly, angiogenesis is particularly prominent in pancreatic endocrine tumors, and the relationship between intratumoral MVD and tumor prognosis seems to be the opposite of that seen in other types of tumors. Indeed, three studies (13–15) of 37, 45, and 82 patients with pancreatic endocrine tumors have shown that low MVD could be an unfavorable histoprognostic factor. Our results support these findings because a higher MVD was observed in the group of benign tumors than in the subgroup of tumors of uncertain behavior and carcinomas (P = .015). In addition, tumor diameter of

more than 2 cm and proliferation index of more than 2% were associated with lower MVD values.

We found a significant correlation between MVD evaluated by using histologic techniques and blood flow assessed by using perfusion CT. The association between MVD and the semiquantitative degree of pancreatic endocrine tumor enhancement at CT has been previously suggested by Rodallec et al (18) in a retrospective study of 44 tumors. Compared with the semiquantitative analysis of enhancement previously reported, the perfusion CT technique we utilized provides reliable and quantitative values and a more accurate assessment of tissue perfusion.

Many investigators have shown that perfusion CT provides an in vivo marker of angiogenesis and can be used for diagnosis, risk stratification, and therapeutic monitoring (23,31–33). Recently, Goh et al (34) showed that functional perfusion measurement can help differentiate between colorectal cancer and diverticulitis. Sahani et al (33) have shown that perfusion parameters differ in hepatocellular carcinoma according to histologic differentiation. In lymphomas, perfusion CT values have been shown to reflect tumor grade at histopathologic examination (35).

Only a few investigators have evaluated perfusion CT in pancreatic tumors. Kubota et al (36) reported that the blood flow in pancreatic adenocarcinomas measured by using xenon CT might help predict response to anticancer drugs.

Whereas conventional multidetector CT can only depict tumor size, vascularity, and the presence of liver metastases in pancreatic endocrine tumors, our results suggest that perfusion CT provides additional quantitative preoperative prognostic factors that could influence therapeutic treatment of patients. For example, in patients with small pancreatic tumors located in the head, where benefit of surgery has not been proved, favorable perfusion parameters could suggest follow-up rather than an aggressive approach (37).

Figure 2

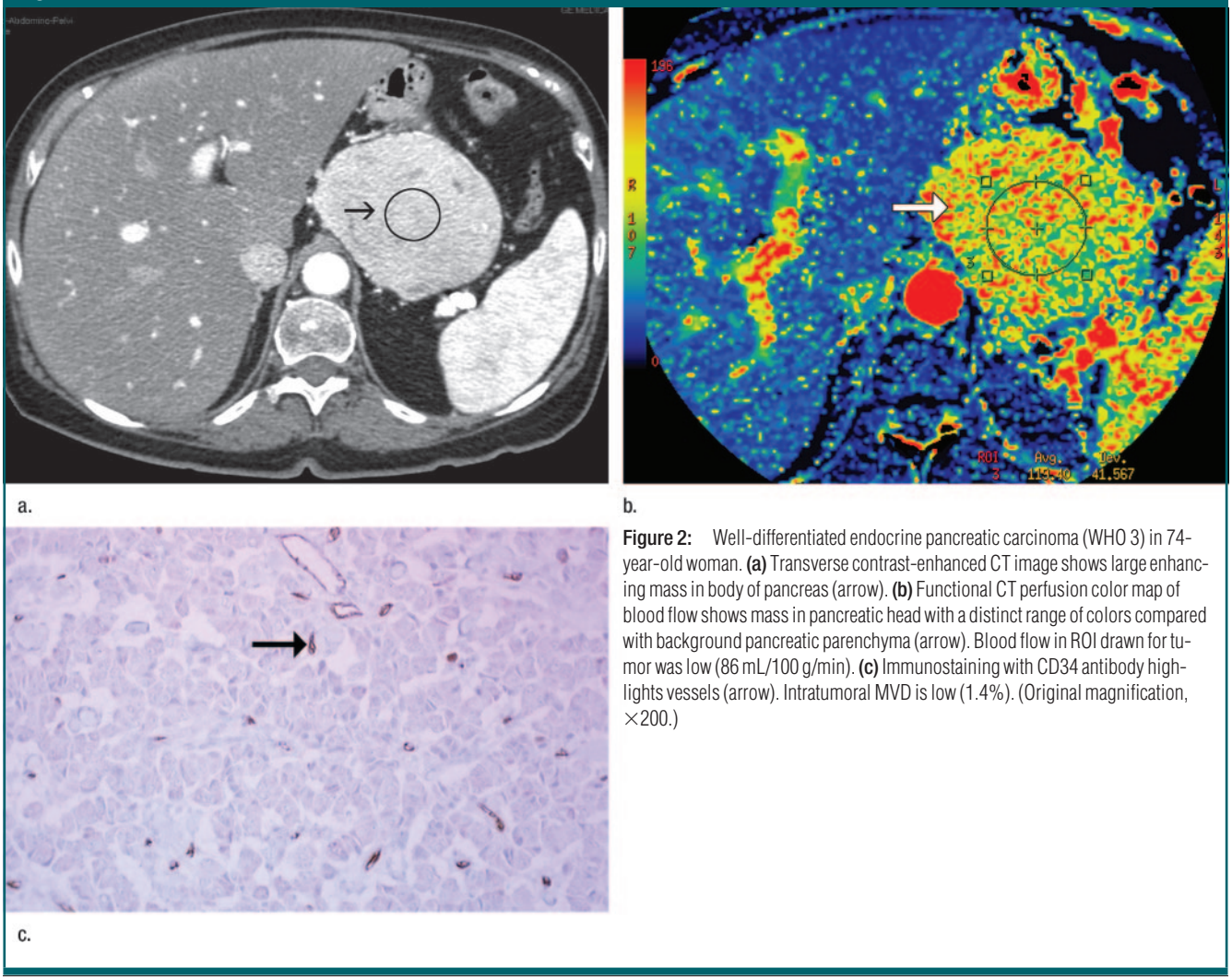

Figure 2: Well-differentiated endocrine pancreatic carcinoma (WHO 3) in 74-year-old woman. **(a)** Transverse contrast-enhanced CT image shows large enhancing mass in body of pancreas (arrow). **(b)** Functional CT perfusion color map of blood flow shows mass in pancreatic head with a distinct range of colors compared with background pancreatic parenchyma (arrow). Blood flow in ROI drawn for tumor was low (86 mL/100 g/min). **(c)** Immunostaining with CD34 antibody highlights vessels (arrow). Intratumoral MVD is low (1.4%). (Original magnification, ×200.)

Our study showed significant differences between blood flow values of benign tumors and tumors of uncertain behavior or well-differentiated carcinomas. Blood flow was higher in WHO 1 tumors than in WHO 2 and 3 tumors. Significant differences in blood flow and mean transit time were also observed on the basis of histoprognostic factors: Blood flow was significantly higher in tumors measuring less than 2 cm in diameter, in those with a proliferation index of 2% or less, and in those without histologic signs of microscopic vascular neoplastic involvement. A longer mean transit time was observed in tumors measuring more than 2 cm in diameter and in those patients with lymph node or liver metastasis. All these results support that, in contrast to most other tumors, the greater the vascularization, the lower the grade in endocrine tumors of the pancreas (13,14,18).

Our study had a number of limitations. Eight of 36 patients were excluded because of motion and beam-hardening artifacts at perfusion CT examination. Beam hardening due to the presence of gas in the stomach and proximal bowel can be limited to some degree by giving water to patients before the examination. Further improvement in the postprocessing algorithm is needed to minimize motion artifacts in the z-axis due to breathing.

Data acquisition was performed at a single tissue level. Whole-tumor assessment with volumetric perfusion measurement has been shown to provide more reliable data (38). Thus, our single section might have been "nonrepresentative" of whole tumor perfusion, especially in large and heterogeneous lesions. However, at pathologic examination, the tumors were sampled in the same axis as the axial CT section, thus facilitating radiopathologic correlation.

Furthermore, in this study, we did not investigate the reproducibility of the postprocessing perfusion measurements. Nevertheless, authors of prior studies have found this to be acceptable, with intraclass correlation greater than 0.8 (39).

The perfusion CT examination conferred an additional effective dose of 10 mSv, which corresponds to the relevant organ radiation dose delivered at an adult abdominal CT examination (40). On the other hand, perfusion CT examination performed as a first step of diagnostic abdominal CT does not require any additional volume of intravenous contrast medium to be administered.

The presence of a selection bias in our study must be noted. We had no WHO 4 grade tumors in our population because those are considered unresectable. Indeed, our work was based on radiopathologic correlation with surgical specimens. Biopsy specimens, which pose the problem of sample variability, are the only material available in WHO 4 grade tumors. Further studies are needed to address this issue in this group of patients.

Last, no long-term follow-up in patients has been performed to assess direct prognostic value of perfusion parameters. Further studies are needed to address this point.

In conclusion, we show that perfusion CT is feasible in patients with pancreatic endocrine tumors and allows evaluation of tumor angiogenesis. It is strongly correlated with histoprognostic factors, such as WHO classification and proliferation index.

By providing an in vivo marker of angiogenesis, perfusion CT may improve our understanding of tumor physiology. It may also provide prognostic information about patient outcomes, help target treatment, and help monitor response to novel therapies.

Acknowledgment: The authors thank Nathalie Colnot.

References

1. Klöppel G, Heitz PU, Capella CES. Endocrine tumours of pancreas. In: Solcia E, Klöppel G, Sobin LH, eds. World Health Organization international histological classification of tumours: histological typing of endocrine tumours. 2nd ed. New York, NY: Springer-Verlag, 2000; 56–60.
2. Heitz PU, Komminoth P, Perren A, et al. World Health Organization classification of tumours. In: DeLellis R, Lloyd R, Heitz PU, Eng C, eds. Pathology and genetics of the tumours of endocrine organs. Lyon, France: IARC, 2004; 175–280.
3. Terris B. Endocrine tumors of the pancreas: classification, clinical and molecular prognostic factors [in French]. Ann Pathol 2002; 22:367–374.
4. Gentil Perret A, Mosnier JF, Buono JP, et al. The relationship between MIB-1 proliferation index and outcome in pancreatic neuroendocrine tumors. Am J Clin Pathol 1998; 109:286–293.
5. La Rosa S, Sessa F, Capella C, et al. Prognostic criteria in nonfunctioning pancreatic endocrine tumours. Virchows Arch 1996;429: 323–333.
6. Rindi G, Kloppel G, Alhman H, et al. TNM staging of foregut (neuro)endocrine tumors: a consensus proposal including a grading system. Virchows Arch 2006;449:395–401.
7. Bergers G, Benjamin LE. Tumorigenesis and the angiogenic switch. Nat Rev Cancer 2003; 3:401–410.
8. Dumortier J, Ratineau C, Roche C, Lombard-Bohas C, Chayvialle JA, Scoazec JY. Angiogenesis and endocrine tumors [in French]. Bull Cancer 1999;86:148–153.
9. Stafford-Johnson DB, Francis IR, Eckhauser FE, Knol JA, Chang AE. Dual-phase helical CT of nonfunctioning islet cell tumors. J Comput Assist Tomogr 1998;22:335–339.
10. Procacci C, Carbognin G, Accordini S, et al. Nonfunctioning endocrine tumors of the pancreas: possibilities of spiral CT characterization. Eur Radiol 2001;11:1175–1183.
11. Horton KM, Hruban RH, Yeo C, Fishman EK. Multi-detector row CT of pancreatic islet cell tumors. RadioGraphics 2006;26:453–464.
12. Fox SB. Tumour angiogenesis and prognosis. Histopathology 1997;30:294–301.
13. Marion-Audibert AM, Barel C, Gouysse G, et al. Low microvessel density is an unfavorable histoprognostic factor in pancreatic endocrine tumors. Gastroenterology 2003;125: 1094–1104.
14. Couvelard A, O'Toole D, Turley H, et al. Microvascular density and hypoxia-inducible factor pathway in pancreatic endocrine tumours: negative correlation of microvascular density and VEGF expression with tumour progression. Br J Cancer 2005;92:94–101.
15. Takahashi Y, Akishima-Fukasawa Y, Kobayashi N, et al. Prognostic value of tumor architecture, tumor-associated vascular characteristics, and expression of angiogenic molecules in pancreatic endocrine tumors. Clin Cancer Res 2007;13:187–196.
16. Miles KA, Griffiths MR. Perfusion CT: a

worthwhile enhancement? Br J Radiol 2003; 76:220–231.

17. Lee TY, Purdie TG, Stewart E. CT imaging of angiogenesis. Q J Nucl Med 2003;47:171–187.
18. Rodallec M, Vilgrain V, Couvelard A, et al. Endocrine pancreatic tumours and helical CT: contrast enhancement is correlated with microvascular density, histoprognostic factors and survival. Pancreatology 2006;6:77–85.
19. Sahani DV, Kalva SP, Hamberg LM, et al. Assessing tumor perfusion and treatment response in rectal cancer with multisection CT: initial observations. Radiology 2005;234: 785–792.
20. Jinzaki M, Tanimoto A, Mukai M, et al. Double-phase helical CT of small renal parenchymal neoplasms: correlation with pathologic findings and tumor angiogenesis. J Comput Assist Tomogr 2000;24:835–842.
21. Tateishi U, Nishihara H, Watanabe S, Morikawa T, Abe K, Miyasaka K. Tumor angiogenesis and dynamic CT in lung adenocarcinoma: radiologic-pathologic correlation. J Comput Assist Tomogr 2001;25: 23–27.
22. Willett CG, Boucher Y, di Tomaso E, et al. Direct evidence that the VEGF-specific antibody bevacizumab has antivascular effects in human rectal cancer. Nat Med 2004;10:145–147.
23. Miles KA. Perfusion CT for the assessment of tumour vascularity: which protocol? Br J Radiol 2003;76(spec no 1):S36–S42.
24. Johnson JA, Wilson TA. A model for capillary exchange. Am J Physiol 1966;210:1299–1303.
25. Abe H, Murakami T, Kubota M, et al. Quantitative tissue blood flow evaluation of pancreatic tumor: comparison between xenon CT technique and perfusion CT technique based on deconvolution analysis. Radiat Med 2005;23:364–370.
26. Xue HD, Jin ZY, Liu W, Wang Y, Zhao WM. Perfusion characteristics of normal pancreas and insulinoma on multi-slice spiral CT [in Chinese]. Zhongguo Yi Xue Ke Xue Yuan Xue Bao 2006;28:68–70.
27. Weidner N, Folkman J, Pozza F, et al. Tumor angiogenesis: a new significant and independent prognostic indicator in early-stage breast carcinoma. J Natl Cancer Inst 1992;84:1875–1887.
28. Vermeulen PB, Verhoeven D, Hubens G, et al. Microvessel density, endothelial cell proliferation and tumour cell proliferation in human colorectal adenocarcinomas. Ann Oncol 1995;6:59–64.
29. Ellis LM, Takahashi Y, Fenoglio CJ, Cleary KR, Bucana CD, Evans DB. Vessel counts and vascular endothelial growth factor expression in pancreatic adenocarcinoma. Eur J Cancer 1998;34:337–340.
30. Duarte IG, Bufkin BL, Pennington MF, et al. Angiogenesis as a predictor of survival after surgical resection for stage I non-small-cell lung cancer. J Thorac Cardiovasc Surg 1998; 115:652–658.
31. Cenic A, Nabavi DG, Craen RA, Gelb AW, Lee TY. A CT method to measure hemodynamics in brain tumors: validation and application of cerebral blood flow maps. AJNR Am J Neuroradiol 2000;21:462–470.
32. Purdie TG, Henderson E, Lee TY. Functional CT imaging of angiogenesis in rabbit VX2 soft-tissue tumour. Phys Med Biol 2001;46: 3161–3175.
33. Sahani DV, Holalkere NS, Mueller PR, Zhu AX. Advanced hepatocellular carcinoma: CT perfusion of liver and tumor tissue—initial experience. Radiology 2007;243:736–743.
34. Goh V, Halligan S, Taylor SA, Burling D, Bassett P, Bartram CI. Differentiation between diverticulitis and colorectal cancer: quantitative CT perfusion measurements versus morphologic criteria—initial experience. Radiology 2007;242:456–462.
35. Dugdale PE, Miles KA, Bunce I, Kelley BB, Leggett DA. CT measurement of perfusion and permeability within lymphoma masses and its ability to assess grade, activity, and chemotherapeutic response. J Comput Assist Tomogr 1999;23:540–547.
36. Kubota M, Dono K, Hashimoto K. Evaluation between tissue blood flow of pancreatic cancer and therapeutic effect of chemoradiation therapy with Xenon CT [in Japanese]. Presented at the 58th annual meeting of the Japanese Society of Gastroenterological Surgery, Sapporo, Japan, July 2003.
37. Falconi M, Plockinger U, Kwekkeboom DJ, et al. Well-differentiated pancreatic nonfunctioning tumors/carcinoma. Neuroendocrinology 2006;84:196–211.
38. Hakime A, Peddi H, Hines-Peralta AU, et al. CT perfusion for determination of pharmacologically mediated blood flow changes in an animal tumor model. Radiology 2007;243: 712–719.
39. Sanelli PC, Nicola G, Tsiouris AJ, et al. Reproducibility of postprocessing of quantitative CT perfusion maps. AJR Am J Roentgenol 2007;188:213–218.
40. Brenner DJ, Hall EJ. Computed tomography: an increasing source of radiation exposure. N Engl J Med 2007;357:2277–2284.